

# NOVEL TEMPORAL FOURIER-TRANSFORM SPECKLE PATTERN SHEARING INTERFEROMETER

C. Joenathan\*, B. Franze, P. Haible, and H. J. Tiziani  
Universitaet Stuttgart, Institut fuer Technische Optik,  
Pfaffenwaldring 9, 70569 Stuttgart,  
Germany

Keywords: Interferometry, Speckle Phenomena, Nondestructive testing, Speckle shearing

**Abstract:** A method to measure derivatives of displacement using time variation changes in the object together with Fourier-transform analysis in speckle shear interferometry is aimed in this paper. The concept of the method is that the object is deformed continuously and a number of sheared images of the object motion are acquired using a high speed CCD camera. The derivative of the object deformation is then retrieved from this large set of data using Fourier-transformation. The method is capable of obtaining information for object displacements over 1000 microns a very difficult task when using conventional electronic speckle pattern shearing interferometry. Theory as well as some of the experimental results with the new method is delineated in this paper.

\*Permanent address: Department of Physics and Applied Optics, Rose-Hulman Institute of Technology, 5500 Wabash Avenue, Terre-Haute, IN 47803, USA. C. J. is a visiting Humbolt fellow.

## 1. Introduction:

Speckle shearing method is a powerful tool for deformation measurements because of its variable sensitivity and ease of experimental arrangement [1-4]. Several shearing mechanisms have been proposed to overcome different problems encountered in the experimental arrangement but the basic principle of operation of all these methods are the same. The popular method of shearing is by using two mirrors and a beam splitter, and by tilting one of the mirrors two images of the object one displaced with respect to the other are produced. Essentially the displacement at one object point is compared to a neighboring point on the same object, thereby producing slope information about the object deformation. Electronic processing of the speckle shearing system is Electronic Speckle Pattern Shearing Interferometry (ESPSI). Some of the shearing mechanisms are Billet split lens [5], bi-prism [6,7], and gratings [8].

The purpose of this paper is to report an alternative method for analyzing the sheared speckle pattern by using a Fourier-transform method. From a series of frames of the sheared images collected as the object is deformed, the

object slope is extracted. In the ESPSI system usually the number of fringes used for analysis is kept low for higher accuracy, which means object displacement is of the order of few tens of microns. However, object deformation much greater than few tens of microns can also be studied by reducing the sensitivity that is by reducing the shear. On the other hand we show that for large shears, the technique we are proposing can measure large object deformation ranging from few tens of microns to few hundreds of microns. In fact we have measured deformations of 1000  $\mu\text{m}$ . The range of deformation measurement is dependent on the instrumentation, magnitude of the shear, and the correlation between the time delayed speckle patterns. Recently we also proposed a Fourier-transform technique to measure large object displacements using speckle interferometry [9] where deformations over 100  $\mu\text{m}$  were determined. Earlier work using the Fourier transformation method of analysis [10] was for measuring absolute step height and object shapes called Fourier-transform speckle topography with wavelength shift [11,12].

In this paper, we describe the principle behind the method and then present some experimental results. Some limitations of this

method along with possible solutions are also presented.

## 2. Theory:

The schematic of the Fourier-transform speckle pattern shearing interferometric method is shown in Fig. 1. Light from a laser is expanded and collimated, and a beam splitter  $BS_1$  is used to illuminate the object along the direction of its normal. The back-scattered beam from the object is then directed to the photo sensor of a high speed Charge Coupled Device (CCD) camera using a beam splitter  $BS_2$  and two mirrors  $M_1$  and  $M_2$ . A telecentric system is used for imaging the object. Two images of the object are obtained from the two mirrors and they can be displaced in the image plane by tilting either one of them.

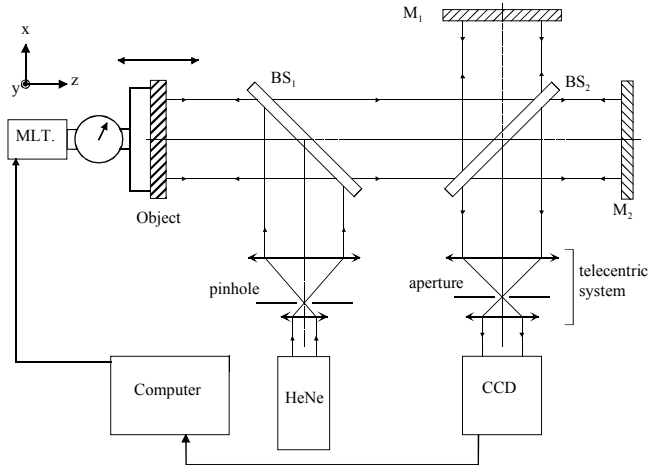


Fig. 1: Schematic experimental arrangement of the Fourier-transform speckle pattern shearing interferometric method;  $BS_1$  and  $BS_2$  are beam splitters, MLT is the linear motorized translation stage which is computer controlled, and  $M_1$  and  $M_2$  are mirrors.

Unlike in conventional interferometry or speckle interferometry where the object profile is compared to a plane reference beam, in speckle shearing interferometry a point in the object surface is compared to an adjacent point on the same object. Especially in our method of analysis, the relative temporal displacements of the two object points are compared. At the plane of the sensor, the intensity at a point on the image can be expressed as

$$I(x, y, t) = I_0(x, y) \left\{ 1 + V \cos \left[ \Phi_0(x, y) + \Phi_0(x, y) + \frac{4\pi [W(x, y, t) - W(x + \Delta x, y + \Delta y, t)]}{\lambda} \right] \right\} \quad (1)$$

Where  $I_0(x, y)$  is the bias intensity of the speckle pattern,  $V$  is the visibility of the speckle modulation,  $\Phi_0(x, y)$  is the random phase,  $W(x, y, t)$  is the displacement at an object point  $(x, y)$ ,  $W(x + \Delta x, y + \Delta y, t)$  is the displacement at another object point  $(x + \Delta x, y + \Delta y)$ , and  $W$  is the z-component of the displacement. At a given instant of time in the object deformation, the modulation that is being observed is due to the relative displacements and can be shown to be the slope along the x-axis at the point  $(x, y)$  and is  $dW(x, y, t)/dx$ . The sensitivity of the speckle shearing interferometric system in our arrangement because of the illumination lies along the z-direction. Let us consider one speckle on the image of the object and as the object is deformed the intensity fluctuation is recorded as a function of time. If the deformation is kept linear then the intensity fluctuation due to the relative displacements is sinusoidal with one frequency. Assuming that the object deformed  $\Delta W(x, y, t)$  distance in 't' seconds, then the temporal frequency of the signal observed at a given point of the object is

$$f(x, y) = \frac{2 \frac{\partial W(x, y, t)}{\partial x} \Delta x}{\lambda t} \quad (2)$$

This shows that the temporal frequency of the signal observed at different points on the object is different if the slope is different. We record a series of frames of the speckle pattern as the object is being displaced linearly. Each frame is then a record of the relative intensities of two speckles at an instant of time. For each pixel we observe their variation over time rendering the fluctuations of the speckle as the object was being deformed which we call the pixel history. This oscillation in the total intensity of two speckles is the temporal frequency at a given pixel. By taking the Fourier-transform of each pixel history, two peaks are obtained on either side from the center peak in the frequency plane for a signal of single temporal frequency. The separation of one peak from the center can be used to determine the slope of the deformation. In this method of analysis

the lower limit on the temporal frequency is chosen such that three peaks in the Fourier spectrum are separated. Moreover, temporal frequency should not be greater than the Nyquist frequency, which is half the number of the frames. Finally using a band-pass filter, one of the side order peaks is filtered and an inverse Fourier-transform is applied to the filtered frequency spectrum. The phase is then unwrapped as in phase shifting interferometry and thereby a 3-D map of the time dependent phase can be generated. The final phase can be expressed as

$$\Phi(x, y) = \Phi_0(x, y) + \frac{4\pi \frac{\partial W(x, y)}{\partial x} \Delta x}{\lambda} \quad (4)$$

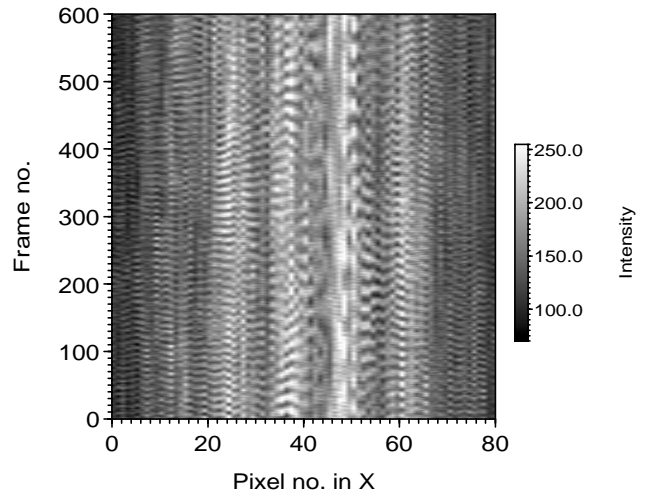
Where  $\Phi_0(x, y)$  is the initial phase, which is usually a constant. Essentially the instantaneous angular frequency or the relative linear acceleration generated during deformation of the object point is determined. From these extrapolations the 3-D plot of the object slope can be extracted.

### 3. Experimental Procedure and Results:

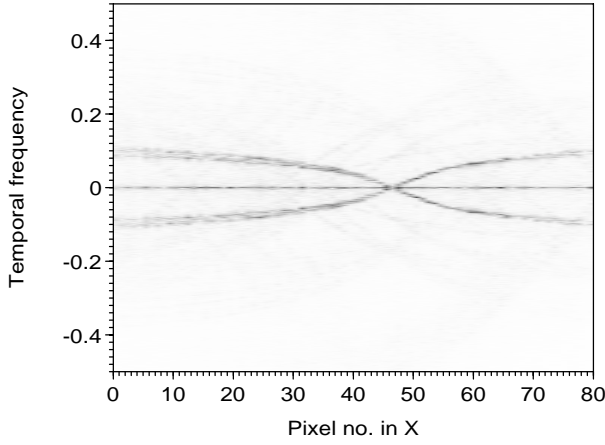
A He-Ne laser beam with a power of 4 mW was expanded with a spatial filtering set up and then collimated to obtain a beam of 30mm diameter. Two images of the object are obtained using a Michelson interferometer. One of the mirrors was slightly tilted to displace one image along the x-axis for example by 2.0 mm at the object plane. The aperture in the telecentric system placed at the focal length of the first lens was adjusted to make the speckle size to be the same if not greater than the pixel size. The rate of object deformation was then determined to get at least 120 cycles and more. The high speed CCD camera can normally be used to acquire 820 frames in one second. However, frame rate was reduced down to 360 frames per second to maintain higher sensitivity of the camera. Acquisition of the 1024 frames as well as the deformation of the object was synchronized.

A plate clamped along its edges and loaded at the center was used as our object of study to test this method. A plastic sheet of 1.5 mm thickness was cut to a circular shape of around 65mm with a clear aperture of 60 mm and clamped uniformly along its edges. In order to increase the light that is

back scattered a retro-reflective tape was taped on one side of the plastic sheet. The object was then point loaded at the center with the tip of a dial gauge whose scale reading can be read to one  $\mu\text{m}$  accuracy. The dial gauge was then loaded with a step-up motor operated linear translation stage (MSL) where the speed of translation and the distance of translation were synchronized with data acquisition. The distance of translation was determined so that not more than 512 cycles was obtained during data acquisition of three seconds. In order to obtain one constant frequency the data was usually acquired after few seconds of loading. From a series of trials the technique was found to be robust and immune to external light and disturbances. Figure 2 (a) shows the modulation of a horizontal line of pixels observed over the three seconds of deformation. Little over half the frames are shown to illustrate modulation. A one dimensional FFT on the horizontal line of 128 pixels stacked to 1024 frames was taken and Fig. 2 (b) shows the separation of the transform peak in the frequency domain as a function of the object point coordinate. The separation of the peaks gradually reduces from one end and reaches zero at the point of loading. The peaks change signs after the point of loading which agrees very well with the theory for such an object.



(a)

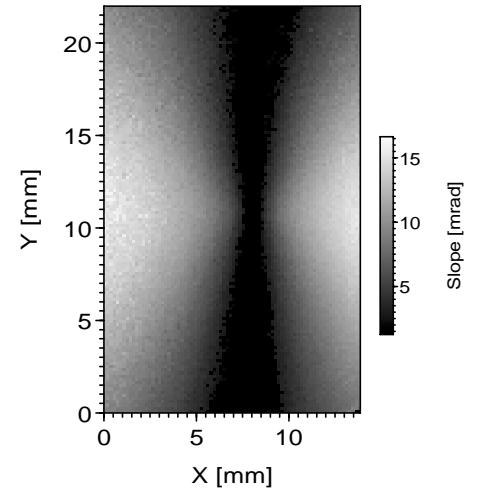


(b)

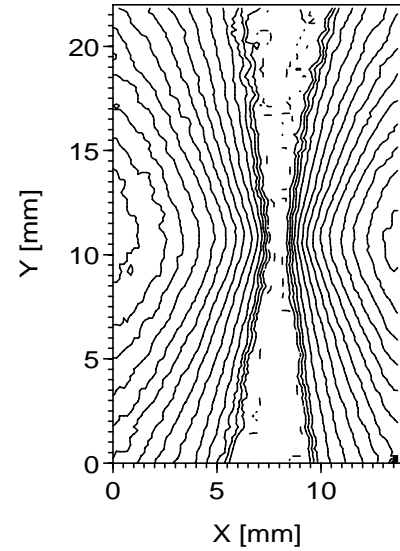
Fig. 2: Experimental results with the circular diaphragm clamped along the edges. The diaphragm was loaded to 300  $\mu\text{m}$  and the shear at the object plane was 2.0 mm. The area of observation was 12 x 20  $\text{mm}^2$ . a) Shows the slice of one horizontal line of pixel from each frame stacked together. Only 600 of the 1024 frames are shown to clearly depict the speckle modulation. b) Two dimensional Fourier-transformation of the temporal signal shown in (a). The separation of the peaks reduces and becomes zero at the point of loading.

As stated before, the Fourier-transform method can be used if the twin peaks that appear from the central peak are separated. However, it can be clearly seen that the peaks close to the center of loading cannot be resolved and therefore no data is obtained. Also for points on the object that do not produce resolvable modulations have no slope data. In our particular case of the choice of the object, points in and around a vertical line passing through the point of loading have no slope value. However, slope values for the points away from the point of loading can be obtained from a shear in the y-direction. Therefore, for points that are close to the loading tip, no slope data is obtained.

Figure 3 a) shows the 3-D plot of the slope of the object deformation in a 12 x 20 mm area with the point of loading at the center of the object. The center of the object was loaded to 550  $\mu\text{m}$  and the shear at the object plane was 2.0mm. The contour plot is shown in Fig. 3 b). A relative good agreement between theory and the experimental results were obtained. The slope values at the point where no data was obtained were set to zero.



(a)



(b)

Fig. 3: Shows the slope data processed using Fourier-transform techniques. The points where no data was obtained was eliminated. a) The 3-D plot of the slope that is expressed in mrad. b) Contour plot of the slope data. Each contour line corresponds to a slope change of 1.12 mrad.

#### 4. Discussions:

Speckle decorrelation reduces the modulation and especially for large deformation the modulation gradually reduces. However, the modulation reappears if the object is further deformed or displaced. The correlation of the speckles was increased by a telecentric system with a low aperture. Further, in the analysis, the width of the band-pass filter offers the possibility to measure

slopes while small changes in frequency are automatically eliminated during the filtering process.

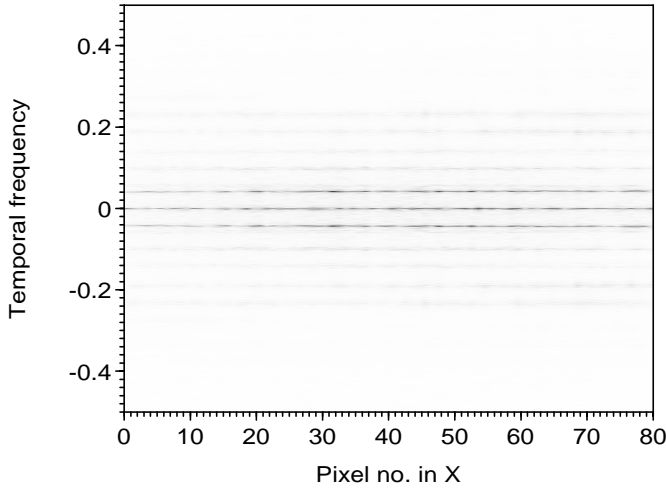


Fig. 4: Shows the results of the two dimensional Fourier-transform of the data when the object was tilted at the rate of 0.1 degree per second.

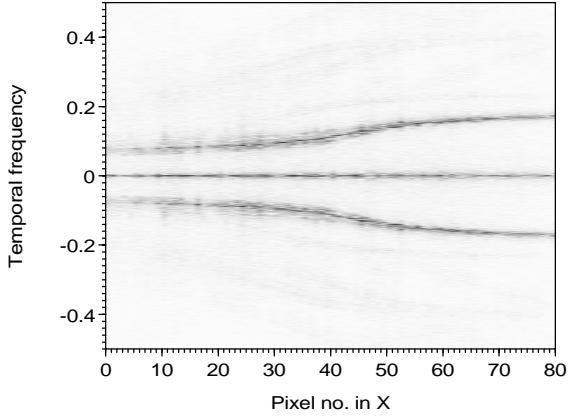
The separation of the peaks in the frequency spectrum is related to the slope changes of the object thereby points on the object with no slope cannot be resolved. Also for points where the slope is close to zero, no resolvable separation of the peaks in the spectrum is obtained. This resolution is dependent on the band-pass filter used to separate one of the side order peaks. However if the frequency scanning method is used, then at least one period within the frame sequence is needed to estimate the slope.

To solve this problem it is helpful to add a constant frequency to the FFT spectra so as to push the peaks at the negative frequency values well over the positive values. Thus data over the whole area of observation was obtained. The constant frequency was generated by tilting the object with a constant angular velocity. Figure 4 shows the constant frequency obtained by tilting the object. If shear is along the x-axis, the object has to be tilted about the y-axis and vice versa for y-axis shear. For small tilts change of the size of the object that is analyzed is negligible. The Fourier-transform was applied to one horizontal line from a frame and stacked over the 1024 frames. This constant frequency obtained with tilting the object while it is being deformed can be employed to separate the peaks. The tilt of the object along with deformation modifies equation 1 to

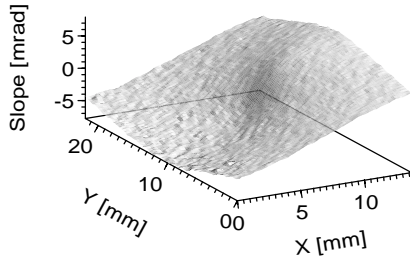
$$I(x, y, t) = I_0(x, y) \left\{ 1 + V \cos \left[ \phi(x, y) + \frac{4\pi}{\lambda} \frac{\partial W'}{\partial x} \Delta x + \frac{4\pi}{\lambda} \frac{\partial W(x, y, t)}{\partial x} \Delta x \right] \right\} \quad (4)$$

Where  $dW'/dx$  is the constant slope generated by tilting the object. The same object was investigated now with a continuous tilt. Figure 5 a) shows the separation of the peaks with the introduction of a tilt as the object is being deformed. In this plot higher orders that are in multiples of the original frequency but of very low amplitude are observed. This is due to the beam splitter that was used in the shearing system. The thickness of the glass plate is such that it matches the shear used and therefore larger shear is introduced from these weak reflections, thus resulting in the higher order peaks. The deformation as well as the tilting of the object was synchronized with data acquisition. One can see that the tilting of the object has to be such that the highest frequency with negative values must be pushed to positive values. The 3-D plot of the deformation is shown in Fig. 5 b) along with the contour plot in Fig. 5 c). Naturally the addition of the constant frequency reduces the maximum deformation that can be measured with this system. The total deformation at the center of the object was 475  $\mu\text{m}$ .

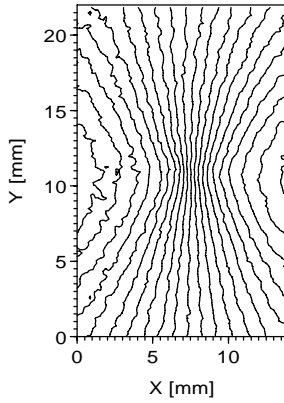
If the deformation is not linear then the process of extracting the data using Fourier-transform method is not possible because the peak is broadened. A simple method of extracting the slope would be to count the number of cycles. Further, as the data is available, the process can be carried out in the region of smaller slope values also. Best results are obtained if there are 120 to 300 cycles in 1024 frames and therefore the total deformation that can be determined is dependent on the magnitude of shear. In our experiments we have deformed the object to about 500  $\mu\text{m}$  for most of the trials.



(a)

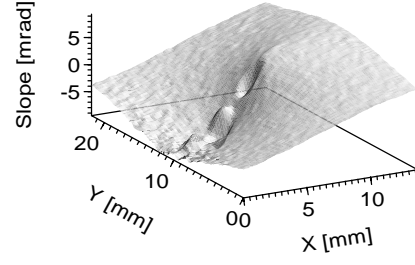


(b)

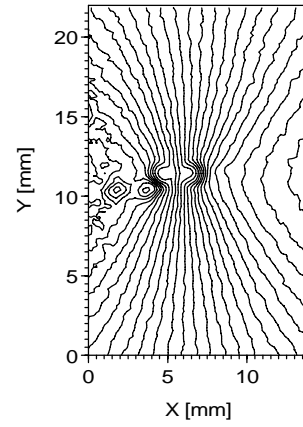


(c)

Fig. 5: Results for the circular diaphragm loaded to  $300\ \mu\text{m}$  as well as tilted continuously at the rate of  $0.3$  degree per second. The rotation was determined so that the peaks with negative values were moved to the positive axis. a) The two dimensional transform shows the separation of the data. b) Shows the 3-D plot of the deformation of the diaphragm filtered with a low pass filter with a  $3 \times 3$  kernel. c) Contour plot of the slope data was also filtered with a  $3 \times 3$  low pass filter. Each contour line corresponds to a change of  $0.53$  mrad.



(a)



(b)

Fig. 6: The middle section of the diaphragm with a defect and an air gap was studied. The object was deformed to a total of  $300\ \mu\text{m}$ . The defect was located close to the center of loading was a small dent and the other very close to it was an air gap between the retro-reflective taps and the diaphragm. The data presented in this figure was filtered with a  $3 \times 3$  low pass filter. a) Shows the 3-D plot of the deformation. b) Shows the contour plots of the slope and the defect as deviations of the contour lines. Each contour line corresponds to a slope change of  $0.77$  mrad.

It is very well known that ESPSI is a powerful tool for nondestructive testing (NDT). In order make the defect appreciable, sometimes large object deformations are necessary. Therefore, in our attempt we deformed the object to around  $1000\ \mu\text{m}$  for some trials. Figure 6 a) and b) shows the 3-D plot and the contour plot for a diaphragm with a defect in the center and on the side. The shear at the object plane for trial was  $2.0\text{mm}$  and the center of the object was deformed to  $575\ \mu\text{m}$ . The defect close to the center of loading was a dent in the diaphragm where the thickness of the diaphragm



was different and the other was air pockets between the retro-reflective tape and the plastic diaphragm. The defects are pronounced in the phase plots as well as the contour plots.

## 5. Conclusions:

We have proposed a new temporal Fourier transform speckle shear pattern interferometer where object displacements in excess of 500  $\mu\text{m}$  can be studied. In some cases the object was deformed to over 1000  $\mu\text{m}$ . Using a high speed CCD camera a large number of frames of the object that is being deformed were acquired. In principle one can use a standard CCD camera to collect the data. The deformation results in generating a sinusoidal signal whose frequency is not only related to the wavelength of light used but also the shear value. The sinusoidal frequency is obtained from each pixel by stacking the 1024 frames. This data was then analyzed by Fourier-transform techniques where one of the side peaks was then isolated by a band-pass filter. One problem associated with this method is the regions with no slope or low slope values. A solution to this problem was achieved by tilting the object as the data is being acquired. The results suggest the high usability of this method for NDT analysis.

## Acknowledgment:

The authors gratefully acknowledge the financial support by the 'German Research Association' DFG and the Alexander von Humboldt foundation.

## 6. References:

1. R. K. Erf, *Speckle Metrology*, Academic Press, New York, 1978
2. R. Jones and C. Wykes, "Holographic and Speckle Interferometry," Cambridge University Press, London, 1983
3. R. S. Sirohi, "Speckle Metrology," Marcel Dekker, New York, 1993
4. C. Joenathan, "Speckle Photography, Shearography, and ESPI," in *Optical methods for testing*, ed. P. Rastogi, R. Tech, London, 1997
5. R. Krishnamurthy, R. S. Sirohi, and M. P. Kothiyal, "Speckle shearing interferometry; a new method," *Applied Optics*, 21, 2065-2067 (1982)
6. Y. Y. Hung, I. M. Daniel, and R. E. Rowlands, "Full-field optical strain measurement having post-recording sensitivity and directional selectivity," *Experimental Mechanics*, 18, 56-60 (1978)
7. S. Nakadata, T. Yatagai, and H. Saito, "Digital speckle pattern shearing interferometry," *Applied Optics*, 19, 4241-4246 (1980)
8. C. Joenathan and L. Buekle, "Electronic Speckle Pattern Shearing Interferometer using holographic gratings," *In Press Optical Engineering* (1997)
9. C. Joenathan, B. Franze, P. Haible and H. J. Tiziani, "A new Fourier-transform speckle interferometric method for measuring large object deformation," *Communicated to Applied Optics* (1997)
10. M. Takeda, H. Ina, and S. Kobayashi, "Fourier-transform method of fringe pattern analysis for computer-based topography and interferometry," *J. Opt. Soc. Am*, 72, 156-160 (1982)
11. H. Tiziani, B. Franze, and P. Haible, "Wavelength-shift speckle interferometry for absolute profilometry using a mode-hop free external cavity diode laser," *J. Mod. Opt*, 44, 1485-1496 (1997)
12. M. Takeda and H. Yamamoto, "Fourier-transform speckle profilometry: three-dimensional shape measurements of diffuse object with large height steps and/or spatially isolated surfaces," *Applied Optics*, 33, 7829-7837 (1994)